JOURNAL OF SOLID STATE CHEMISTRY 32, 41–50 (1980)

Phase Equilibria for the System $Fe_{0.394}$–$Ti_{0.606}$–O–S at 1380 and 1485 K

IAN E. GREY AND RICHARD R. MERRITT

CSIRO Division of Mineral Chemistry, P.O. Box 124, Port Melbourne, Victoria 3207, Australia

Received December 15, 1978; in revised form June 18, 1979

This paper reports equilibrium phase data for the system $Fe_{0.394}$–$Ti_{0.606}$–O–S under reducing conditions. The work was part of a wider study of equilibrium phase data relevant to a commercial reduction process for upgrading ilmenite. The iron to titanium ratio was chosen to approximate closely that of the altered ilmenite feed used by Western Titanium Ltd at their upgrading plant at Capel in Western Australia. The system was studied at 1380 and 1485 K using the equilibration and quench technique, with the sulfur and oxygen fugacities in the gaseous atmosphere independently controlled by use of mixtures of hydrogen, hydrogen sulfide, and carbon dioxide. The results are presented on log f_{S_2} *vs* log f_{O_2} isothermal phase diagrams, which are discussed in terms of the relevant subsystems Fe–Ti–O, Fe–S, and Fe–S–O. Thermodynamic data measured for the four-component system generally agree with those published for the Fe–Ti–O and Fe–S systems.

1. Introduction

Western Titanium Ltd operate an ilmenite upgrading plant at Capel in Western Australia (*1*). Their process uses high temperature reduction of the ilmenite to metallic iron and titanium-rich oxides. The iron is removed from these oxides by accelerated corrosion using the Becher process (*2*). It was previously shown (*3, 4*) that the 1 to 2 wt% of manganese, which is an impurity in the ilmenite feed, lowers the titanium content of the upgraded product. However, this impurity effect can be partly overcome by adding sulfur to the reduction (*5*). To understand why sulfur is beneficial it is necessary to know the phase equilibria in the five-component system Fe–Mn–Ti–O–S at the conditions of the commercial reduction. This paper reports the first step in determining this information, that is, phase equilibria in the quaternary subsystem $Fe_{0.394}$–$Ti_{0.606}$–O–S at 1485 and 1380 K. The measured data are applicable to the maximum and minimum temperature at which reduction occurs in the plant, and the iron to titanium ratio closely approximates that of the altered ilmenite feed.

The equilibration and quench method was used with independent control of the sulfur and oxygen fugacities. The ranges of fugacities studied at 1485 K were for sulfur $10^{-5.8}$ to $10^{-3.9}$ atm, and for oxygen $10^{-16.0}$ to $10^{-11.9}$ atm. At 1380 K the sulfur fugacities ranged from $10^{-6.3}$ to $10^{-4.9}$ atm, and the oxygen fugacities from $10^{-17.1}$ to $10^{-13.2}$ atm.

2. Previous Work

2.1. The Fe–Ti–O Subsystem

There is no reported literature on the Fe–Ti–O–S system relevant to the present work, but useful data are available from studies of the subsystems Fe–Ti–O, Fe–O–S, and Fe–S.

0022-4596/80/040041-10$02.00/0

For the ternary oxide system, Merritt and Turnbull (*6*) collated the published data and presented phase diagrams at the two temperatures 1273 and 1473 K. In general the equilibrium phase assemblages in these two diagrams are similar, but they differ under conditions where the iron is partially reduced and the ratio titanium to total metal is greater than 0.5. The two-phase assemblage pseudobrookite solid solution and metallic iron, $M_3O_5 + Fe_m$, which occurs at the higher temperature is unstable at 1273 K and is replaced by the assemblage ilmenite solid solution and rutile, $M_2O_3 + MO_2$. Saha and Biggar (*7*) estimated that the minimum temperature for stability of the $M_3O_5 + Fe_m$ assemblage was 1353 ± 10 K.

The fixed oxygen fugacities for the three-phase equilibria $M_2O_3 + M_3O_5 + Fe_m$ and $M_3O_5 + MO_{2-x} + Fe_m$ at 1473 K were shown by Grey *et al.* (*4*) to be $10^{-13.05}$ and $10^{-13.95}$ atm, respectively. The former value agrees well with Merritt and Turnbull's mean figure of $10^{-13.07}$ atm (*6*).

2.2. The Fe–S and Fe–S–O Subsystems

For the experimental conditions used in the present work, Bale and Toguri (*8*) and Stofko *et al.* (*9*) showed that only metallic iron and a liquid iron sulfide with variable sulfur content could exist in the FeS system at 1473 K. Naldrett (*10*) summarized the data for the Fe–O–S system at 1473 and 1393 K. His Figs. 11 and 12 show that at the experimental fugacities used in the present study (see Section 1), the oxygen content of the liquid iron sulfide would range from less than 0.5 wt% up to a maximum of 3.5 wt% and that no other oxysulfide phase would be stable.

For the binary system Rosenqvist (*11*) established that the sulfur fugacity for the metallic iron/liquid sulfide equilibrium was $10^{-5.44}$ atm at 1473 K and $10^{-6.04}$ atm at 1373 K. The former figure was confirmed by Bale and Toguri (*8*) who obtained an equilibrium sulfur fugacity of $10^{-5.40}$ atm at 1473 K.

2.3. Other Systems

There are no published data for the Ti–O–S system relevant to the present study. However, the results of Abendroth and Schlechten (*12*) for the Ti–S system combined with thermodynamic data for the titanium oxides (*13–16*) clearly show that no titanium sulfides would be expected in equilibrium under the experimental conditions.

3. Experimental

Phase equilibria in the system $Fe_{0.394}$–$Ti_{0.606}$–O–S were determined by the equilibration and quench technique. Pellets of an appropriate mixture of the anatase form TiO_2 and Fe_2O_3 were heated under an atmosphere of controlled sulfur and oxygen fugacities and then quenched under liquid nitrogen. The phases present in the quenched samples were determined by X-ray diffraction. The oxides were Fischer certified reagents which were dried at 1073 K prior to use.

Some additional data were measured for the $Fe_{0.394}$–$Ti_{0.606}$–0 system. For these experiments sulfur was excluded from the equilibrating atmosphere and only the oxygen fugacity was controlled.

3.1. Control of Gas Fugacities

The oxygen and sulfur fagacities were controlled by mixing hydrogen, carbon dioxide, and hydrogen sulfide in ratios which were established by metering the gases through calibrated flow meters. The oxygen and sulfur fugacities were calculated from the gas ratios using the computer program CHEMIX (*17*). The uncertainty in the value of $\log f_{S_2}$ or $\log f_{O_2}$ was estimated to be ± 0.05.

3.2. X-Ray Diffraction

X-Ray powder diffraction patterns were obtained with a Philips diffractometer fitted

with a graphite monochromator using Cu$K\alpha$ radiation.

3.3. Sample Equilibration

X-Ray diffraction patterns for quenched products showed that more than the equilibrium number of phases usually occurred in samples heated at conditions near a phase boundary. In such cases these excess phases could usually be removed by grinding the sample, repelleting, and reheating. The major exception was for samples heated at 1380 K where two boundaries lay very close together. Near these boundaries, even four heatings usually did not completely remove the excess phases. At 1485 K samples were only reheated when excess phases were found or when they were heated at conditions known to be near to phase boundaries. In contrast all samples were routinely reheated in the lower temperature study.

4. Results

4.1. The System $Fe_{0.394}$–$Ti_{0.606}$–O–S at 1485 K

The phases found in the quenched samples are given in Table I. The phase boundaries obtained from this data are shown on the log f_{S_2} *vs* log f_{O_2} plot in Fig. 1. The Gibbs phase rule predicts that under the experimental constraints there will be two condensed phases in equilibrium except at phase boundaries. It is evident from Table I that where the iron sulfide is found so too is metallic iron and an oxide phase. This apparent violation of the phase rule is due to the eutectic decomposition of the liquid sulfide into metallic iron and the troilite form of iron sulfide, which occurs on quenching. Such a decomposition would be expected from the Fe–S phase diagram (*18*) and experimental evidence for it comes from Fig. 2. This is a scanning electron micrograph of a quenched sample which contains troilite, metallic iron, and the oxide M_4O_7. The metallic iron (light gray) always occurs in a matrix of iron

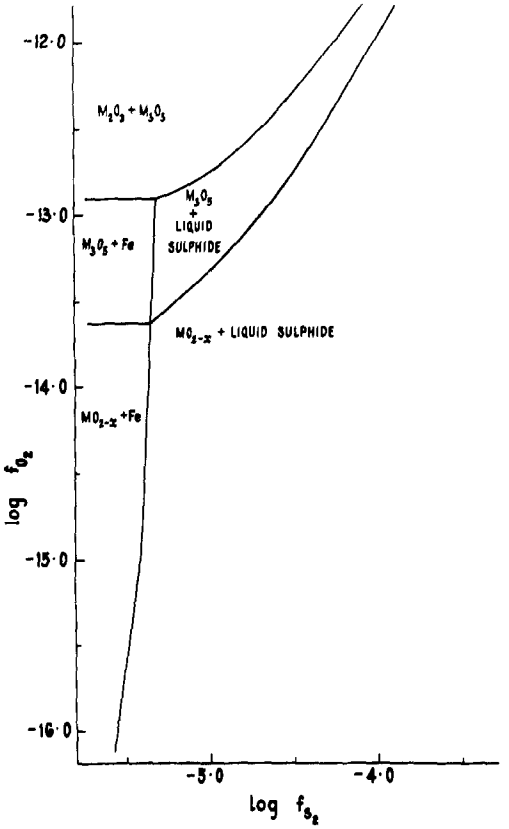

FIG. 1. The equilibrium phase assemblages and phase boundaries for the system $Fe_{0.394}$–$Ti_{0.606}$–O–S at 1485 K on a plot of log f_{S_2} vs log f_{O_2}.

sulfide (mid-gray). At the higher oxygen fugacities, where the liquid would contain a small amount of oxygen, the X-ray diffraction technique was not sufficiently sensitive to reveal whether a third phase resulted from the quenched liquid.

The phase diagram falls into two parts separated by the boundary where metallic iron is sulfidized to liquid iron sulfide. At oxygen fugacities above 10^{-15} atm this boundary is slightly dependent on oxygen fugacity. The mean value of f_{S_2} at the boundary is $10^{-5.35\pm0.05}$ atm. Below $f_{O_2} = 10^{-15}$ atm the oxygen fugacity dependence increases so that at $f_{O_2} = 10^{-16}$ atm iron is sulfidized at $10^{-5.54}$ atm.

In that part of Fig. 1 where metallic iron is stable there are two boundaries which are

TABLE I

PHASES FOUND IN SAMPLES FROM THE $Fe_{0.394}$–$Ti_{0.606}$–O–S SYSTEM AT 1485 K

$\log f_{S_2}$	$\log f_{O_2}$	M_2O_3	M_3O_5	MO_{2-x}	Troilite	Fe
−4.225	−11.900	P[a]	P		?	
−4.147	−11.901	T	P		P	P
−4.042	−11.898		P		P	?
−3.926	−11.896		T	P	P	P
−4.614	−12.260	P	P			
−4.532	−12.276	P	P			
−4.412	−12.227	T	P		T	?
−4.370	−12.270		P		P	P
−4.259	−12.288		?	P	P	P
−4.152	−12.289		?	P	P	P
−3.954	−12.270			P	P	P
−4.944	−12.665	P	P			
−4.841	−12.676		P		P	P
−4.734	−12.631		P		P	P
−4.523	−12.631		P		P	P
−4.456	−12.684		P		P	P
−4.354	−12.671		?	P	P	P
−4.246	−12.647		?	P	P	P
−5.524	−12.863	P	P	?		
−5.547	−12.988		P			P
−5.535	−13.071		P			P
−5.342	−13.104		P			P
−5.249	−13.104		P		P	P
−5.135	−13.035		P		P	P
−4.939	−13.029		P		P	P
−4.843	−13.072		P		P	P
−4.696	−13.014			P	P	P
−4.620	−13.042		?	P	P	P
−4.535	−13.047			P	P	P
−5.162	−13.464		P		P	P
−4.413	−13.409			P	P	P
−5.322	−13.560		P		P	P
−4.469	−13.601			P	P	P
−5.426	−13.656		T	P		P
−5.353	−13.721			P	P	P
−5.630	−13.810			P		P
−5.483	−13.863		P	P		P
−5.391	−13.950		P	P		P
−5.423	−14.139			P		P
−5.438	−14.265			P		P
−5.322	−14.390			P	P	P
−5.502	−14.596			P		P
−5.432	−14.702			P	?	P
−5.341	−14.649			P	P	P
−5.516	−14.998			P		P
−5.426	−14.956			P	T	P
−5.360	−15.000			P	P	P
−5.532	−15.233			P		P
−5.397	−15.185			P	P	P
−5.554	−15.748			P	?	P

TABLE I—continued

PHASES FOUND IN SAMPLES FROM THE $Fe_{0.394}$–$Ti_{0.606}$–O–S SYSTEM AT 1485 K

$\log f_{S_2}$	$\log f_{O_2}$	M_2O_3	M_3O_5	MO_{2-x}	Troilite	Fe
−5.504	−15.678			P	P	P
−5.410	−15.633			P	P	P
−5.772	−16.003			P		P
−5.692	−15.984			P		P
−5.530	−15.954			P	P	P
−5.434	−16.000			P	P	P

[a] Major phases are indicated by the letter P; phases that occur in trace amounts but do show sufficient lines to enable positive identification are indicated by the letter T. Where there are not enough lines to identify a phase without doubt, a question mark is used.

independent of sulfur fugacity. The reaction occurring at both is the metallization of iron from the ternary oxide phases. In reduction the more iron-rich phase, M_2O_3, disappears first at $f_{O_2} = 10^{-12.92}$ atm and then the less iron-rich M_3O_5 phase disappears at $f_{O_2} = 10^{-13.63}$ atm. At oxygen fugacities below $10^{-13.63}$ atm the reduced rutile phases MO_{2-x} are in equilibrium with metallic iron.

At sulfur fugacities where liquid iron sulfide is stable there are two phase boundaries which result from the sulfidation of iron from the ternary oxide phases. As before the M_2O_3 phase disappears at higher oxygen fugacities than the M_3O_5, and following the loss of M_3O_5 the reduced rutile phases are in equilibrium with liquid iron sulfide. These boundaries are functions of both the sulfur and oxygen fugacities.

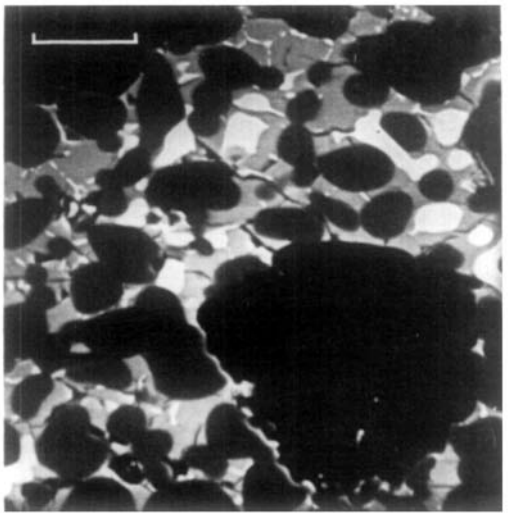

FIG. 2. A scanning electron micrograph showing metallic iron (light gray) within a matrix of the troilite form of iron sulfide (midgray). The dark gray phase is the oxide M_4O_7. (Scale bar = 20 μm.)

4.2. The System $Fe_{0.394}$–$Ti_{0.606}$–O–S at 1380 K

The phases found in the quenched samples at 1380 K are listed in Table II and the equilibrium phase diagram based on these data is given in Fig. 3.

Figure 3 has the same form as the phase diagram at 1485 K. It is separated into two parts by the boundary at $f_{S_2} = 10^{-6.01\pm0.05}$ atm where metallic iron is sulfidized to liquid iron sulfide. This boundary shows a small oxygen fugacity dependence, but unlike the situation at 1485 K the dependence does not increase at low oxygen fugacities. To the left of this boundary two sulfur independent boundaries occur at $f_{O_2} = 10^{-14.44}$ and $10^{-14.56}$ atm corresponding to destabilization of M_2O_3 and M_3O_5, respectively. To the right of the metallic iron/liquid sulfide boundary iron from the ternary oxide phases is sulfidized to liquid sulfide at two boundaries which are functions of both the sulfur and oxygen fugacity.

TABLE II

PHASES FOUND IN SAMPLES FROM THE $Fe_{0.394}$–$Ti_{0.606}$–O–S SYSTEM AT 1380 K

$\log f_{S_2}$	$\log f_{O_2}$	M_2O_3	M_3O_5	MO_{2-x}	Troilite	Fe
−6.026	−14.240	P[a]	P			T
−6.052	−14.368	P	P			P
−6.023	−14.453	T	P			P
−5.902	−14.559		P	P		P
−6.106	−14.562		P	T		P
−6.135	−14.710		T	P		P
−6.069	−15.122			P		P
−6.248	−15.380			P		P
−6.051	−15.579			P		P
−6.056	−16.197			P		P
−6.111	−17.128			P		P
−6.310	−17.145			P		P
−4.909	−14.251	P	T	P		
−4.880	−13.372	P	T	P		
−4.926	−13.492	T	P	P	P	P
−4.943	−13.610	T	P	P	P	
−4.884	−14.020			P	P	P
−5.026	−13.480	P	P	T		
−5.088	−13.480	P	P	T		
−5.311	−13.627	P	P	T		
−5.280	−13.805	P	P	T		
−5.317	−13.908	P	P	T	P	P
−5.305	−14.010			P	P	P
−5.316	−14.137			P	P	P
−5.352	−14.469			P	P	P
−5.546	−13.783	P	P			
−5.754	−14.016	P	P			
−5.778	−14.233	T	P	?	P	P
−5.776	−14.324		P	P	P	P
−5.788	−14.524			P	P	P
−5.962	−15.118			P	P	P
−5.612	−15.342			P	P	P
−5.827	−15.388			P	P	P
−5.976	−15.388			P	T	P
−5.830	−15.538			P	P	P
−5.967	−16.212			P	P	P
−6.008	−17.110			P	P	P

[a] Major phases are indicated by the letter P; phases that occur in trace amounts but do show sufficient lines to enable positive identification are indicated by the letter T. Where there are not enough lines to identify a phase without doubt, a question mark is used.

It was not possible to achieve equilibrium in samples heated at conditions close to the boundaries where iron from the ternary oxide phases is sulfidized or metallized (see Section 3.3). Thus these boundaries are not defined as precisely as those in the remainder of this study.

4.3. Experiments in the $Fe_{0.394}$–$Ti_{0.606}$–O System

To help define the boundaries at low sulfur fugacities, experiments were performed without hydrogen sulfide in the equilibrating atmosphere. The results of these experiments are given in Table III.

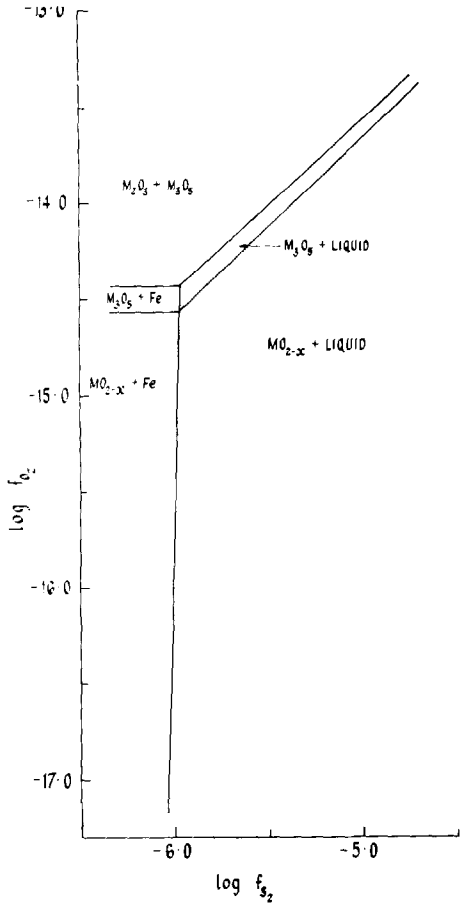

FIG. 3. The equilibrium phase assemblages and phase boundaries for the system $Fe_{0.394}$–$Ti_{0.606}$–O–S at 1380 K on a plot of $\log f_{S_2}$ vs $\log f_{O_2}$.

5. Discussion

The experimental results are best considered in three sections, as follows: first at low oxygen fugacities where the quaternary system behaves as the subsystem Fe–S, second at low sulfur fugacities where the quaternary system behaves as the Fe–Ti–O subsystem, and third at high sulfur and high oxygen fugacities where there is both sulfur and oxygen involvement in the reactions which determine the phase equilibria.

5.1. Comparison of Experimental Results with Those for System Fe–S

The experimental results for the quaternary system show an apparent oxygen fugacity dependence for the metallic iron/liquid sulfide equilibrium. The dependence is small. It is only at 1485 K and at oxygen fugacities below 10^{-15} atm that the difference in sulfur fugacity between that observed for the boundary and the mean figure, $10^{-5.35}$ atm, exceeds the experimental uncertainty. Chemical equilibrium explanations of this effect in terms of the incorporation of sulfur into reduced rutiles or titanium into the sulfide phase at low oxygen fugacities are not supported by chemical analyses. An explanation which is consistent with the sign of the slope is that there is some thermal segregation of hydrogen from the hydrogen sulfide and carbon dioxide at the very high ratios H_2/H_2S and H_2CO_2 which are necessary to achieve the low sulfur and low oxygen fugacities.

Figure 4 is a linear plot of the mean values of the $\log f_{S_2}$ vs $1/T$ for the metallic iron/liquid sulfide equilibrium in the presence of M_3O_5 or MO_{2-x} phases. The plot is extrapolated for comparison with the results of Bale and Toguri (*8*) and Rosenqvist (*11*) for the same equilibrium in the binary system Fe–S. The close agreement between all sets of data in both magnitude and slope of the plot indicates that the oxide phases have a negligible effect on the sulfidation reaction

$$\mathrm{Fe}(c)+\tfrac{1}{2}y\mathrm{S}_2(g)=\mathrm{FeS}_y(l). \qquad (1)$$

5.2. Comparison with Published Results for System Fe–Ti–O

At conditions where the sufide phase is not stable the boundaries between the two-phase assemblages occurred at the same oxygen fugacities whether or not hydrogen sulfide is in the equilibrating atmosphere. Thus under these experimental conditions the quaternary oxide–sulfide system behaves exactly as

TABLE III

RESULTS OF EQUILIBRATION-QUENCH STUDIES IN THE SYSTEM $Fe_{0.394}$–$Ti_{0.606}$–O

Temperature (K)	Oxygen fugacity $\log f_{O_2}$	Phases in quenched samples			
		M_2O_3	M_3O_5	MO_{2-x}	Fe_m
1380[a]	−14.460		P	P	P
1380	−14.460		P		P
1425[b]	−13.659	P	P		
1425	−13.719	P	P		P
1425	−13.793		P		P
1425	−13.863	?	P		P
1425	−14.103		P	?	P
1425	−14.171		P	P	P
1425	−14.225		T	P	P
1485	−12.901	P	P		
1485	−12.971		P		P
1485	−13.593		P		P
1485	−13.645		P	P	P
1485	−13.667			P	P

[a] Starting materials—anatase form TiO_2 + synthetic $FeTiO_3$.

[b] Starting materials—M_3O_5 + Fe, prepared by reacting $Fe_2O_3 + TiO_2$ at 1425 K and at $f_{O_2} = 10^{-13.86}$ atm. All other runs used mixtures of Fe_2O_3 and TiO_2 as starting materials.

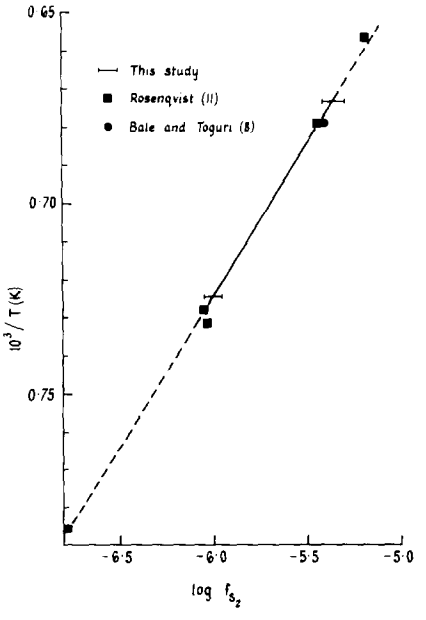

FIG. 4. A plot of $\log f_{S_2}$ vs $1/T$ for the equilibrium between metallic iron and liquid iron sulfide. Data from the present study are compared with published data from the binary system Fe–S.

does the ternary system. The idealized reactions occurring at these boundaries are, respectively,

$$2M_2O_3 = M_3O_5 + Fe_m + \tfrac{1}{2}O_2, \quad (2)$$

$$M_3O_5 = 2MO_2 + Fe_m + \tfrac{1}{2}O_2 \quad (3)$$

Our experimental data for three temperatures are combined in Fig. 5 to give a linear plot of $\log f_{O_2}$ vs $1/T$ for both the three-phase equilibria. Interpolated values of the oxygen fugacity from this diagram may be compared with published data for the ternary system. Our results for the boundary $M_2O_3 + M_3O_5 + Fe_m$ at 1473 K agree with published data of Grey *et al.* (*4*), but for boundary $M_3O_5 + MO_{2-x} + Fe_m$ their value of oxygen fugacity (*4*) is lower than would be predicted by the present results. Since samples heated at oxygen fugacities just below the latter three-phase boundary usually showed M_3O_5 as the major phase when heated once, but confirmed the equilibrium assemblage MO_{2-x} + metallic iron on reheating, it is

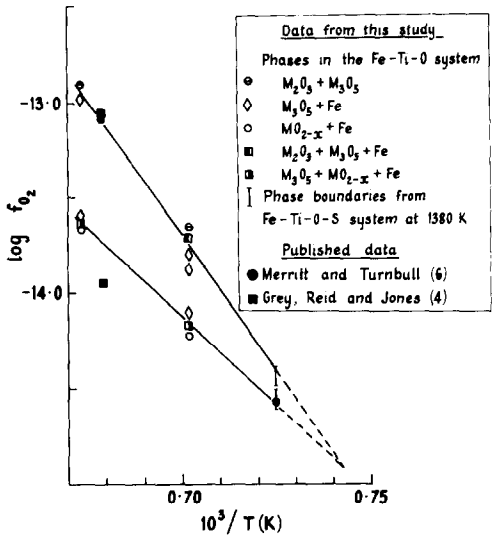

FIG. 5. A plot of $1/T$ vs log f_{O_2} showing the two three-phase boundaries $M_2O_3+M_3O_5+Fe_m$ and $M_3O_5+MO_{2-x}+Fe_m$. These boundaries were defined using data for the system $Fe_{0.394}$–$Ti_{0.606}$–O–S from Table II and for the system $Fe_{0.394}$–$Ti_{0.606}$–O from Table III. For comparison with the present data, the published oxygen fugacities for the phase boundaries at 1380 and 1473 K are shown on this figure.

likely that part of the discrepancy between the two sets of data arises from the presence of metastable M_3O_5.

Figure 3 shows that at 1380 K the oxygen fugacity for the equilibrium $M_3O_5+MO_{2-x}+Fe_m$ is $10^{-14.56}$ atm. This value agrees with the previously published data which are summarized by Merritt and Turnbull (*6*) in their Fig. 2.

The extrapolation of the data of Fig. 5 suggests that the $M_3O_5+Fe_m$ assemblage would exist to 1346 K ($1/T = 0.743\times 10^{-3}$ K^{-1}). For comparison, Saha and Biggar (*7*) obtained the value of 1353 ± 10 K. At temperatures below 1346 K, where the $M_3O_5+Fe_m$ assemblage is unstable, the phase relations are those which Merritt and Turnbull (*6*) described for 1273 K. At temperatures just above 1346 K, the phase relations are more complex than were shown previously (*6*) for 1473 K due to the presence of two miscibility gaps in the M_3O_5 solid solution. We have obtained experimental evidence for this which will be published subsequently.

5.3. Region of High Sulfur and High Oxygen Fugacities

The two boundaries present under conditions of high sulfur and high oxygen fugacity represent equilibrium between the phases $M_2O_3+M_3O_5+$liquid sulfide and $M_3O_5+MO_{2-x}+$liquid sulfide. They are functions of both sulfur and oxygen fugacity, and the idealized equations for the reactions at the boundary are, respectively,

$$2M_2O_3+\tfrac{1}{2}yS_2=FeS_y+M_3O_5+\tfrac{1}{2}O_2 \quad (4)$$

and

$$M_3O_5+\tfrac{1}{2}yS_2=FeS_y+2MO_2+\tfrac{1}{2}O_2. \quad (5)$$

These equations are the sum of those representing the sulfur and oxygen independent reactions; for example, Eq. (4) is the sum of $Fe+\frac{1}{2}yS_2=FeS_y$ and $2M_2O_3=Fe+M_3O_5+\frac{1}{2}O_2$.

If allowance is made for the known compositional variations in the individual phases, the boundary reactions may be written precisely as

$$Fe_aTi_{2-a}O_3+AS_2 = BFeS_bO_c+CFe_dTi_{3-d}O_5+DO_2 \quad (6)$$

and

$$Fe_eTi_{3-e}O_5+ES_2 = FFeS_fO_g+FFe_hTi_{1-h}O_{2-i}+HO_2. \quad (7)$$

It is seen that in Eqs. (6) and (7) all the condensed phases have compositions which depend on both the sulfur and oxygen fugacities, and so the boundaries which the equations represent need not have constant slopes on a log f_{S_2} vs log f_{O_2} phase diagram. The amount of curvature shown in the

boundaries will be determined by the changes that occur in the stoichiometric variables $a, b \ldots i$ as the fugacity is changed. The curvature is clearly seen in Fig. 1 for equilibrium at 1485 K. It is not seen at 1380 K and is possibly obscured by the insufficiently precise definition of the boundaries at the lower temperature (see Section 4.2).

6. Summary

The phase relations applicable to the reduction of altered ilmenite in the system Fe–Ti–O–S were studied under controlled sulfur and controlled oxygen fugacities at 1485 and 1380 K. The results of the study led to the following conclusions:

(1) Over the range of low oxygen fugacities studied, metallic iron sulfidized to liquid iron sulfide at sulfur fugacities which were essentially independent of the titanium oxides which were present at equilibrium. The equilibrium sulfur fugacities from the present data agreed with those published for the binary system, Fe–S.

(2) At sulfur fugacities where liquid iron sulfide is unstable relative to metallic iron, the four-component system behaves as the ternary-oxide system Fe–Ti–O.

(3) The sequence of two-phase assemblages found in reduction of the ternary-oxide with the ratio $[Fe]/[Fe+Ti] = 0.394$ was the same at both 1485 and 1380 K, and this sequence is likely to remain the same down to approximately 1346 K.

(4) At high sulfur and high oxygen fugacities the four-component system behaves as would be predicted by adding the reactions which occur in the subsystems Fe–S and Fe–Ti–O.

References

1. B. F. BRACANIN, P. W. CASSIDY, J. M. MACKAY, AND H. W. HOCKIN, TMS Paper Selection No. A72-31, 209 (1972).
2. R. G. BECHER, Australian Patent 247, 110 (Sept. 1963).
3. I. E. GREY AND A. F. REID, *Inst. Mining Met. Trans. Sect. C* **83**, 39 (1974).
4. I. E. GREY, A. F. REID, AND D. G. JONES, *Inst. Mining Met. Trans. Sect. C* **83**, 105 (1974).
5. P. E. ROLFE, *in* "Western Australia Conference 1973," Australasian Institute of Mining and Metallurgy, Melbourne (1973).
6. R. R. MERRITT AND A. G. TURNBULL, *J. Solid State Chem.* **10**, 252 (1974).
7. P. SAHA AND G. M. BIGGAR, *Indian J. Earth Sci.* **1**, 43 (1974).
8. C. W. BALE AND J. M. TOGURI, *Canad. Met. Quart.* **13**, 463 (1974).
9. M. STOFKO, J. SCHMIEDL, AND T. ROSENQVIST, *Scand. J. Met.* **3**, 113 (1974).
10. A. J. NALDRETT, *J. Petrol.* **10**, 171 (1969).
11. T. ROSENQVIST, *J. Iron Steel Inst. London* **176**, 37 (1954).
12. R. P. ABENDROTH AND A. W. SCHLECHTEN, *Trans. Met. Soc. AIME* **215**, 145 (1959).
13. I. E. GREY, C. LI, AND A. F. REID, *J. Solid State Chem.* **11**, 120 (1974).
14. R. R. MERRITT, B. G. HYDE, L. A. BURSILL, AND D. K. PHILP, *Phil. Trans. Roy. Soc. London Ser. A* **274** 627 (1973).
15. K. SUZUKI AND K. SAMBONGI, *Tetsu To Hagane* **58**, 1579 (1972).
16. S. M. ARIYA, M. D. MOROZOVA, AND E. VOL'F, *Russ. J. Inorg. Chem.* **2**, 16 (1957).
17. A. G. TURNBULL, *in "APCOM* 77," 49–53, *pp. Australasian Institute of Mining and Metallurgy, Melbourne* (1977).
18. M. HANSEN, "Constitution of Binary Alloys," 2nd ed., pp. 704–708. McGraw-Hill, New York, (1958).